Modeling Galactic Dust in CMB B-Mode Observations

Kali Byrnes

May 1, 2026

1 Introduction/Background

The cosmic microwave background (CMB) is leftover radiation from the early universe produced about 380,000 years after the Big Bang. As time progresses, the CMB travels towards us while acting as a snapshot of what the universe looked like at that time of the Big Bang. The CMB allows us to study the origin and evolution of the universe.

The CMB is not perfectly uniform because it has tiny variations in temperature across the sky, referred to as temperature anisotropies, which tell us how matter was distributed in the early universe. In addition to these temperature variations, the CMB light is slightly polarized, which means the light waves have a preferred direction of oscillation, caused by interactions with the matter in the early universe.

These polarization patterns can be separated into two types: E-modes and B-modes. E-modes have a pattern that looks like radial or circular gradients and are relatively well understood by researchers. B-modes, on the other hand, have a swirling, curl-like pattern and are much more difficult to detect and understand. They are especially important because they can contain evidence and information about the primordial gravitational waves from the early universe.

1.1 B-Mode Polarization and Inflation

B-mode polarization is of particular interest because it provides a unique signature of primordial gravitational waves generated during inflation. These tensor perturbations produce a curl-like polarization pattern that cannot be generated by scalar density fluctuations at linear order.

The amplitude of this signal is commonly parameterized by the tensor-to-scalar ratio r, which quantifies the relative strength of primordial gravitational waves. Detecting a nonzero value of r would provide direct evidence for inflation and constrain its energy scale.

1.2 Sources of B-Modes

In practice, the observed B-mode signal is a combination of multiple contributions:

$$C_\ell^{BB} = C_\ell^{BB,\text{primordial}} + C_\ell^{BB,\text{lensing}} + C_\ell^{BB,\text{foreground}} \tag{1}$$

The primordial component is the target signal associated with inflation. The lensing component arises from gravitational deflection of CMB photons by large-scale structure, which converts E-modes into B-modes. The foreground component is dominated by Galactic emission, particularly polarized dust.

At the angular scales of interest for inflationary B-modes, foreground emission is often comparable to or larger than the primordial signal.

1.3 Galactic Dust as a Foreground

Polarized emission from Galactic dust is the dominant foreground at frequencies above approximately 100 GHz. Dust grains align with the Galactic magnetic field and emit polarized radiation, producing both E-mode and B-mode patterns on the sky.

Observations have shown that dust emission can account for a significant fraction of the measured B-mode power, even in relatively clean regions of the sky. As a result, distinguishing between cosmological and foreground signals requires precise modeling of dust emission.

1.4 Multi-Frequency Observations

A key strategy for separating foregrounds from the CMB is to exploit their different frequency dependence. While the CMB follows a nearly perfect blackbody spectrum, dust emission follows a modified blackbody law.

By observing the sky at multiple frequencies, it allows us to disentangle these components through their spectral behavior. For this approach to be successful, it relies on accurate models of how dust emission scales with frequency.

1.5 Challenges in Foreground Modeling

Although parametric models provide a convenient description of dust emission, they rely on simplifying assumptions that may not hold in practice. Dust properties such as temperature, spectral index, and polarization fraction vary across the sky. These variations can lead to differences in frequency scaling between regions, introducing complexity that is not captured by a simple separable model. In particular, the assumption of perfect correlation between frequencies may break down, leading to decorrelation effects that bias parameter estimation.

1.6 Objective of This Work

The goal of this work is to evaluate the validity of the parametric dust model using simulated data. We generate multi-frequency sky maps using the PySM framework and compute B-mode power spectra across several observing bands. By comparing the simulated spectra to the parametric model, we assess whether the model accurately captures the behavior of realistic dust emission. This analysis provides insight into the limitations of simple foreground models and their impact on the search for primordial B-mode polarization.

2 Parametric Description of Dust Emission

The primary objective of this work is to determine whether a simple parametric model can accurately describe polarized Galactic dust emission in CMB B-mode observations. This question is central to modern cosmology, as Galactic foregrounds are known to dominate over the expected primordial B-mode signal across all relevant observing frequencies.

2.1 B-Mode Measurements and Foregrounds

B-mode polarization provides a unique probe of primordial gravitational waves generated during inflation. Unlike E-modes, B-modes cannot be produced by scalar density perturbations at linear order, making them a clean signature of tensor modes.

However, Galactic foregrounds introduce significant contamination. In particular, polarized thermal dust emission produces B-mode patterns that can mimic or dominate the cosmological signal. Observations have shown that dust emission alone can explain much of the observed B-mode power in certain frequency bands. Therefore, separating dust from the cosmological signal requires accurate modeling of its frequency and angular behavior.

2.2 Angular Power Spectrum Representation

The statistical properties of the polarization field are described using angular power spectra:

$$C_\ell^{\nu_1\times\nu_2} = \langle a_{\ell m}^{(B,\nu_1)} a_{\ell m}^{(B,\nu_2)*} \rangle \tag{1}$$

This quantity measures the variance of B-mode fluctuations at angular scale ℓ.

The multipole ℓ corresponds to angular scales on the sky, with larger ℓ representing smaller angular features.

To facilitate interpretation, the spectra are expressed as:

$$D_\ell = \frac{\ell(\ell+1)}{2\pi} C_\ell \tag{2}$$

This form approximately flattens the spectrum and allows for clearer comparison across scales.

2.3 Parametric Dust Model

The dust power spectrum is modeled using a separable parametric form:

$$D_\ell^{\nu_1\times\nu_2} = A_d \, f(\nu_1) f(\nu_2) \left(\frac{\ell}{\ell_*}\right)^\alpha \tag{3}$$

This model assumes that angular dependence and frequency dependence can be treated independently. The amplitude A_d sets the overall power level, while the exponent α describes how the power varies with angular scale.

The functions $f(\nu)$ encode the frequency scaling of dust emission. This separable form is widely used in experimental analyses because it reduces the complexity of foreground modeling to a small number of physically interpretable parameters.

2.4 Frequency Dependence of Dust Emission

Thermal dust emission follows a modified blackbody spectrum:

$$S_\nu = A_d \left(\frac{\nu}{\nu_0}\right)^{\beta_d} B_\nu(T_d) \tag{4}$$

where $B_\nu(T_d)$ is the Planck function, β_d is the spectral index, and T_d is the dust temperature. Typical values are $\beta_d \approx 1.5$ and $T_d \approx 20\,\mathrm{K}$, though both vary across the sky.

This frequency dependence leads to a strong increase in emission amplitude at higher microwave frequencies. As a result, multi-frequency observations are essential for separating dust from the cosmological signal.

2.5 Assumptions and Limitations

The model in Equation (3) relies on several key assumptions:

- The angular and frequency dependence are separable
- Dust properties are uniform across the observed region
- Cross-frequency correlations are perfectly described by $f(\nu_1)f(\nu_2)$

In reality, these assumptions are not strictly valid. Galactic dust exhibits spatial variation in temperature, spectral index, and polarization properties. These variations can lead to decorrelation between frequencies, meaning that cross-spectra cannot be perfectly predicted by a simple separable model.

2.6 Motivation for Simulation-Based Testing

Given these complexities, it is necessary to test the parametric model against realistic sky simulations. The Python Sky Model (PySM) provides a framework for generating multi-frequency maps of Galactic emission based on observational constraints and physically motivated models.

By comparing the parametric model to power spectra derived from PySM simulations, we can evaluate whether the simplified description in Equation (3) is sufficient to capture the behavior of realistic dust emission.

3 Simulated Maps and Power Spectra

To test the validity of the parametric dust model, we generate simulated sky maps using the Python Sky Model (PySM). PySM provides full-sky realizations of Galactic emission based on both observational data and theoretical modeling.

3.1 Overview of PySM

PySM is designed to simulate microwave emission from multiple astrophysical components, including dust, synchrotron radiation, and free-free emission. It produces maps of the Stokes parameters (I, Q, U) at arbitrary frequencies, allowing for direct comparison with CMB observations.

For this analysis, we use the D10 dust model, which incorporates spatial variations in dust amplitude and frequency scaling consistent with observational constraints.

3.2 Simulation Setup and Map Properties

Maps are generated at five frequencies:

$$\nu = \{95,\ 150,\ 220,\ 270,\ 353\}\ \text{GHz}$$

These frequencies correspond to typical observing bands used in experiments targeting B-mode polarization.

As a representative example, Figure 1 shows the simulated polarization maps at 220 GHz.

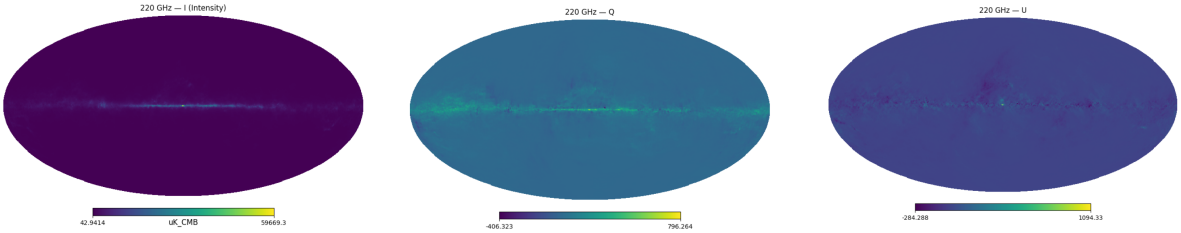

Figure 1: Simulated dust emission maps at 220 GHz showing Stokes parameters I, Q, and U. The total intensity (I) map highlights the overall dust emission, while Q and U form the linear polarization structure. These maps serve as the basis for constructing B-mode power spectra in the analysis.

Similar structure is observed across all frequencies, with amplitude increasing at higher frequencies due to the modified blackbody spectrum of dust emission.

Each simulated map contains the Stokes parameters:

$$I: \text{ total intensity}$$
$$Q, U: \text{ linear polarization components}$$

Dust emission is inherently polarized due to alignment of dust grains with the Galactic magnetic field. This produces polarization fractions up to $\sim 20\%$, with polarization oriented perpendicular to the magnetic field direction.

The simulated maps exhibit strong frequency dependence. Higher-frequency maps show significantly larger amplitudes due to the modified blackbody spectrum of dust emission.

This behavior is consistent with observational data and reflects the rapid increase of dust emission with frequency in the microwave regime.

3.3 Sky Masking

To mimic realistic observations, a sky mask is applied to isolate a localized region. The mask reduces contamination from bright Galactic regions and minimizes edge effects. The mask is smoothly tapered/apodized to suppress artificial mode coupling in harmonic space.

The effect of the mask on the data is illustrated in Figure 2.

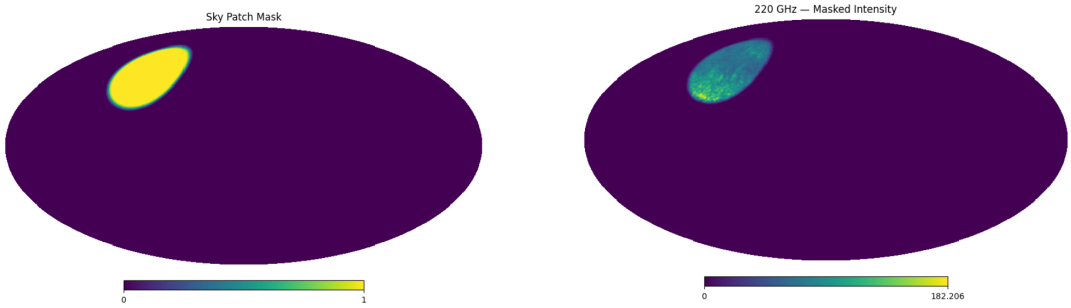

Figure 2: Left: Apodized sky mask used to isolate a low-foreground region of the sky. The mask smoothly transitions to zero at the boundaries to reduce edge effects in harmonic space. Right: Example of the mask applied to the 220 GHz polarization map (Stokes Q). Regions outside the mask are suppressed, leaving only the selected sky area for power spectrum analysis.

Applying the mask reduces contamination from bright Galactic regions and ensures that the subsequent harmonic analysis is restricted to a clean and well-defined sky area.

3.4 Power Spectrum Estimation

The masked maps are transformed into spherical harmonic space:

$$a^T_{\ell m}, a^E_{\ell m}, a^B_{\ell m} = \mathrm{SHT}[I, Q, U] \tag{5}$$

This decomposition separates the polarization field into E-mode and B-mode components. Only the B-mode coefficients are used for subsequent analysis.

The B-mode power spectra are computed for all pairs of frequencies:

$$C_\ell^{\nu_i \times \nu_j} = \langle a^{(i)}_{\ell m} a^{(j)*}_{\ell m} \rangle \tag{6}$$

With five frequencies, this produces a total of 15 spectra, including both auto-spectra and cross-spectra. Cross-spectra provide information about correlations between frequencies and are essential for testing the separability assumption in the parametric model.

The spectra are converted to:

$$D_\ell = \frac{\ell(\ell+1)}{2\pi} C_\ell \tag{7}$$

and binned over the range:

$$30 \leq \ell \leq 380, \quad \Delta\ell = 20$$

Binning reduces noise and yields stable estimates of the power spectrum.

3.5 Observed Features of the Spectra

The resulting spectra exhibit several important features:

- Strong frequency dependence consistent with dust emission

- Significant correlation between frequency bands
- Approximate power-law behavior in ℓ

These features provide a direct test of the parametric model introduced in Section 2. The B-mode power spectra computed from the simulated maps are shown in Figure 3.

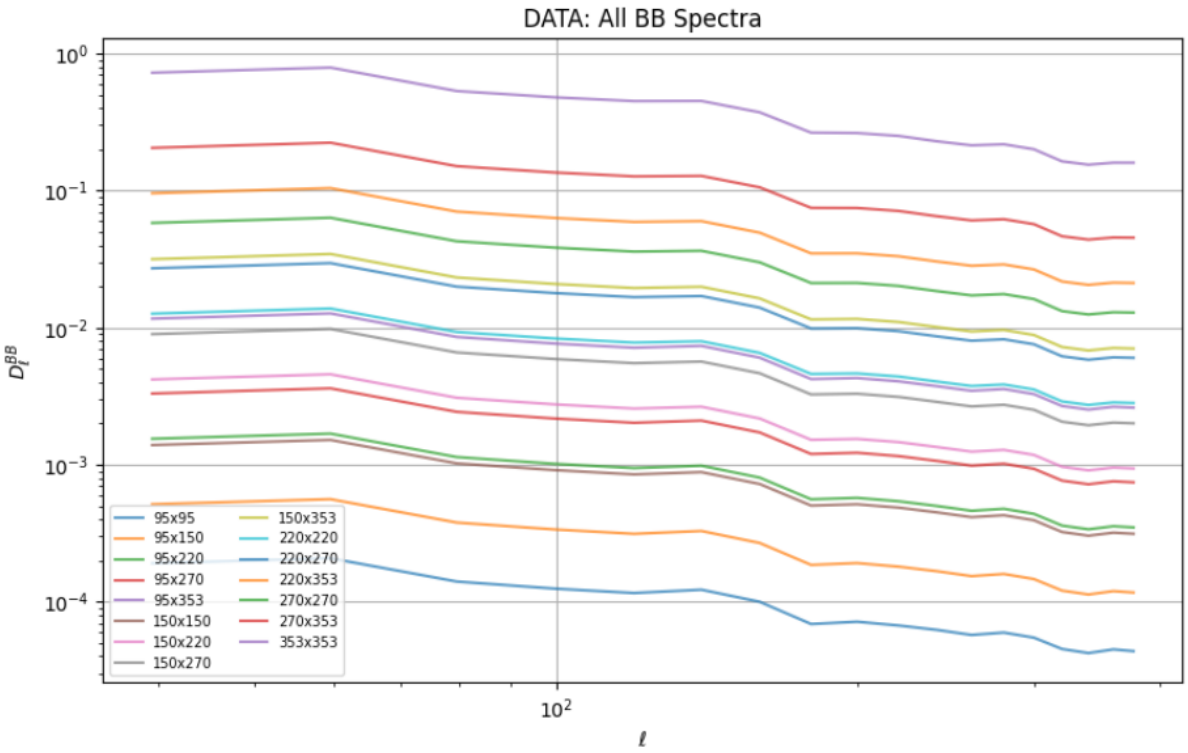

Figure 3: B-mode power spectra $D_\ell^{\nu_i \times \nu_j}$ computed from the simulated maps for all frequency combinations. The spectra exhibit strong frequency dependence and approximate power-law behavior in multipole ℓ, consistent with expectations for Galactic dust emission.

The binned spectra obtained here form the dataset used for parameter estimation and model fitting in the following section.

4 Model Fitting and Parameter Estimation

The objective of this section is to determine whether the parametric dust model introduced in Section 2 provides an accurate description of the simulated power spectra derived in Section 3. This is achieved by fitting the model to the data and quantifying the agreement using a chi-square statistic.

4.1 Model Prediction

The theoretical model for the dust B-mode power spectrum is given by

$$D_\ell^{\nu_1 \times \nu_2} = A_d \, f(\nu_1) f(\nu_2) \left(\frac{\ell}{\ell_*} \right)^\alpha \tag{1}$$

This model predicts the power spectrum for each pair of frequencies and each multipole ℓ. The parameters to be determined are:

$$
\begin{aligned}
A_d &: \text{ dust amplitude} \\
\alpha &: \text{ angular scaling exponent} \\
\beta_d &: \text{ spectral index (via } f(\nu))
\end{aligned}
$$

The function $f(\nu)$ encodes the frequency dependence of dust emission and is derived from the modified blackbody spectrum.

The corresponding model predictions are shown in Figure 4.

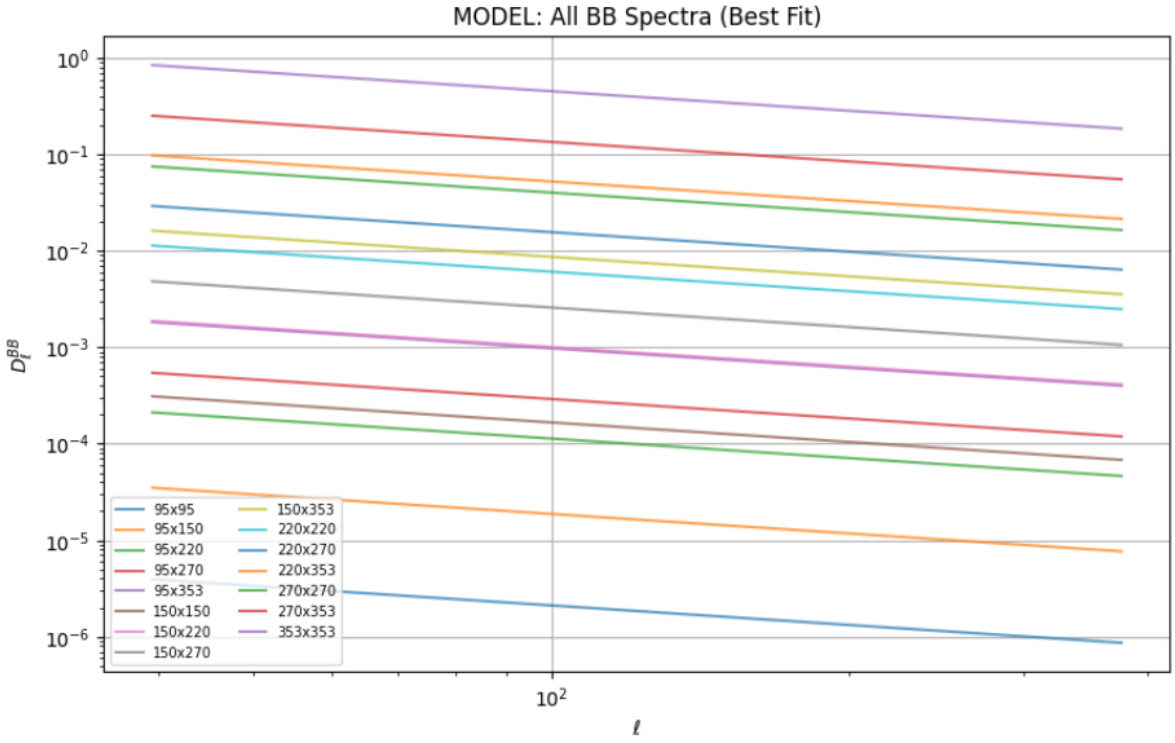

Figure 4: Best-fit parametric model predictions for the B-mode power spectra. The model reproduces the overall amplitude and angular scaling of the spectra under the assumption of separable frequency and multipole dependence.

4.2 Data Vector Construction

The measured data consist of binned power spectra for all frequency pairs. With five frequency maps, this provides 15 spectra, each evaluated over N_{bin} multipole bins.

These spectra are combined into a single data vector:

$$\mathbf{d} = \begin{bmatrix} D_{\ell_1}^{(1)} \\ D_{\ell_2}^{(1)} \\ \vdots \\ D_{\ell_N}^{(15)} \end{bmatrix} \tag{2}$$

The ordering is chosen such that all spectra for a given multipole bin are grouped together. This matches the structure of the covariance matrix used in the analysis. The model predictions are arranged into a corresponding vector $\mathbf{m}$ with the same ordering.

4.3 Chi-Square Definition

The goodness of fit between the data and the model is quantified using the chi-square statistic:

$$\chi^2 = (\mathbf{d} - \mathbf{m})^T \Sigma^{-1} (\mathbf{d} - \mathbf{m}) \tag{3}$$

Here, Σ is the covariance matrix, which encodes the uncertainties and correlations between the data points. This expression measures the weighted squared difference between the data and the model. A smaller value of χ^2 indicates better agreement.

4.4 Covariance Matrix

The covariance matrix accounts for both signal and noise contributions. In general, it is given by

$$\Sigma_{ij} = \frac{2}{k} \left(C_\ell^{ac} C_\ell^{bd} + C_\ell^{ad} C_\ell^{bc} \right) \tag{4}$$

where k represents the number of modes in each multipole bin and depends on the sky fraction and bin width.

This expression reflects the fact that power spectrum estimates are correlated and subject to cosmic variance. In practice, constructing the full covariance matrix is computationally intensive. As an initial approximation, the covariance matrix is taken to be the identity matrix:

$$\Sigma = I \tag{5}$$

This assumes that all data points are independent and equally weighted. While this approximation neglects correlations, it provides a useful starting point for testing the model.

4.5 Parameter Estimation

The best-fit parameters are obtained by minimizing the chi-square function:

$$\hat{\theta} = \arg\min_{\theta} \chi^2(\theta) \tag{6}$$

where $\theta = (A_d, \beta_d, \alpha)$ represents the set of model parameters.

This minimization is performed using a nonlinear optimization algorithm. The parameter space is explored iteratively until the value of χ^2 is minimized.

4.6 Interpretation of Fit Results

The quality of the fit is assessed by comparing the model predictions to the data.

A direct comparison between the simulated spectra and the best-fit model is shown in Figure 5.

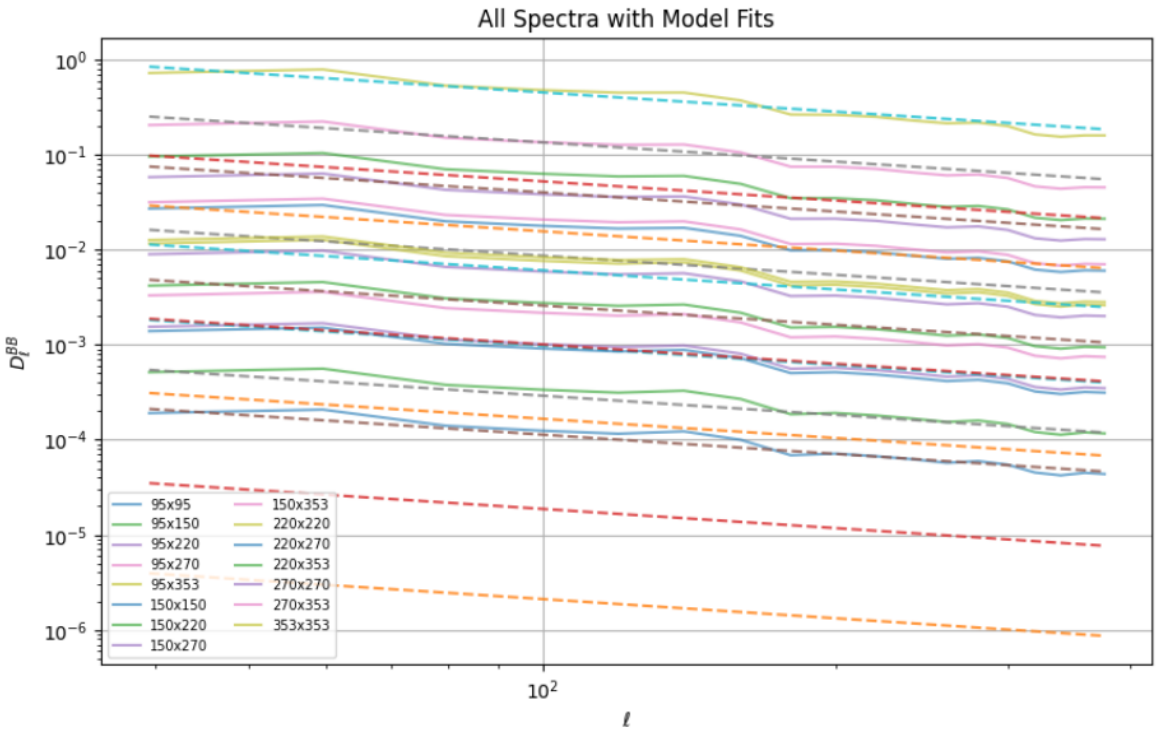

Figure 5: Comparison between simulated B-mode power spectra (solid lines) and best-fit model predictions (dashed lines). While the model captures the overall trends in amplitude and angular scaling, systematic deviations are visible, particularly for widely separated frequency pairs, indicating limitations of the separable parametric model.

If the parametric model accurately describes the simulated spectra, the residuals

$$\mathbf{r} = \mathbf{d} - \mathbf{m} \tag{7}$$

should be small and randomly distributed.

Systematic deviations in the residuals indicate that the model fails to capture certain features of the data. In particular, deviations may arise due to:

- spatial variation in dust properties
- imperfect frequency scaling
- decorrelation between frequency bands

4.7 Limitations of the Fitting Procedure

Several limitations affect the accuracy of the parameter estimation:

- The covariance matrix is approximated as the identity matrix
- Noise and cosmic variance are not fully modeled
- The model assumes perfect separability between frequency and angular dependence

These limitations can lead to biased parameter estimates and underestimation of uncertainties. Nevertheless, this approach provides a clear test of whether the parametric model captures the dominant behavior of the simulated dust spectra.

4.8 Summary

The fitting procedure described in this section provides a quantitative framework for evaluating the parametric dust model. By minimizing the chi-square statistic, we determine the parameters that best reproduce the simulated power spectra.

The results of this analysis allow us to assess whether a simple parametric model is sufficient to describe realistic dust emission, or whether more complex modeling is required.

5 Decorrelation Effects

The parametric model introduced in Section 2 assumes that dust emission is perfectly correlated across observing frequencies. In this section, we examine the validity of this assumption and investigate the presence of decorrelation effects in the simulated data.

5.1 Definition of Frequency Correlation

For two observing frequencies ν_1 and ν_2, the degree of correlation between their B-mode signals can be quantified using the ratio:

$$\rho_\ell^{\nu_1\times\nu_2} = \frac{C_\ell^{\nu_1\times\nu_2}}{\sqrt{C_\ell^{\nu_1\times\nu_1}\, C_\ell^{\nu_2\times\nu_2}}} \tag{1}$$

This quantity is bounded between -1 and 1. If the emission is perfectly correlated between frequencies, then $\rho_\ell = 1$.

In the parametric model of Equation (3) in Section 2, this ratio is implicitly assumed to be equal to unity for all ℓ and frequency pairs.

5.2 Physical Origin of Decorrelation

In realistic environments, dust properties vary across the sky, different regions may have different temperatures, spectral indices, and polarization orientations. These variations lead to differences in the frequency scaling of emission across the sky. As a result, maps at different frequencies are not perfectly correlated. This effect is known as decorrelation and represents a breakdown of the separability assumption in the parametric model.

5.3 Modeling Decorrelation

A commonly used model describes decorrelation as a function of frequency separation:

$$\rho^{\nu_1 \times \nu_2} = \exp\left[-\frac{1}{2}\Delta_d \left(\log \frac{\nu_1}{\nu_2}\right)^2\right] \tag{2}$$

Here, Δ_d is a parameter that quantifies the level of decorrelation. If $\Delta_d = 0$, then $\rho = 1$ and the emission is perfectly correlated. Larger values of Δ_d correspond to stronger decorrelation. This form reflects the expectation that decorrelation increases with the separation between frequencies.

5.4 Measurement from Simulated Data

Using the power spectra computed in Section 3, the correlation coefficient $\rho_\ell^{\nu_1 \times \nu_2}$ is evaluated for all frequency pairs. If the parametric model is valid, these values should be close to unity across all multipoles. Deviations from unity indicate that the cross-spectra are not fully described by the product of frequency scalings, and therefore that the model in Equation (3) is incomplete.

5.5 Implications for Model Accuracy

Decorrelation has important consequences for foreground modeling. If the correlation between frequencies is less than unity, then the simple separable model

$$D_\ell^{\nu_1 \times \nu_2} \propto f(\nu_1) f(\nu_2)$$

no longer provides an exact description of the data.

This leads to systematic errors in parameter estimation, particularly when combining data from widely separated frequency bands. In the context of B-mode searches, even small levels of decorrelation can bias constraints on primordial gravitational waves.

5.6 Interpretation

The presence or absence of decorrelation in the simulated data provides a direct test of the assumptions underlying the parametric model. If decorrelation is weak, then the model provides a good approximation to the data. If decorrelation is significant, more complex models that account for spatial variation in dust properties are required.

5.7 Summary

This section demonstrates that frequency decorrelation is a key limitation of simple parametric models of dust emission. By quantifying the correlation between frequency bands, we assess whether the separability assumption holds. The results provide insight into the level of complexity required for accurate foreground modeling in CMB B-mode analyses.

6 Conclusion

In this work, we investigated whether a simple parametric model can accurately describe polarized galactic dust emission in the context of CMB B-mode measurements. Using simulated sky maps generated with the PySM framework, we constructed multi-frequency B-mode power spectra and compared them to a separable model of the form

$$D_\ell^{\nu_1\times\nu_2} = A_d\, f(\nu_1) f(\nu_2) \left(\frac{\ell}{\ell_*}\right)^\alpha .$$

The simulated spectra exhibit key features expected from dust emission, including strong frequency dependence and approximate power-law scaling in multipole. These trends are broadly consistent with the assumptions of the parametric model.

To quantify this agreement, we performed a chi-square minimization to determine the best-fit model parameters. The results indicate that the model captures the dominant behavior of the spectra, particularly the overall amplitude and angular scaling. However, residuals reveal systematic deviations that cannot be fully explained within the separable framework.

A primary source of these deviations is frequency decorrelation. By examining cross-spectra between frequency bands, we find that the correlation coefficient is not strictly unity, indicating that dust emission does not scale identically across frequencies. This effect arises from spatial variation in dust properties such as temperature, spectral index, and polarization structure.

The presence of decorrelation highlights a fundamental limitation of simple parametric models. While such models provide a useful first-order description of foregrounds, they fail to capture the full complexity of Galactic emission. In particular, the assumption of perfect separability between angular and frequency dependence breaks down in realistic scenarios.

These findings have important implications for CMB experiments. Accurate detection of primordial B-modes requires precise modeling of foregrounds across multiple frequencies. Even small mismatches between the model and the true sky can lead to biased estimates of cosmological parameters.

Future work should focus on incorporating more realistic models of dust emission that allow for spatial variation and partial frequency decorrelation. This may include extending the parametric framework or adopting simulation-based approaches that better capture the underlying physics.

In summary, the parametric dust model provides a reasonable approximation to simulated data but is not sufficient for high-precision analyses. Understanding and modeling decorrelation effects will be essential for detection of primordial gravitational waves in future CMB experiments.

References

[1] D. Samtleben, S. Staggs, and B. Winstein, *The Cosmic Microwave Background for Pedestrians: A Review for Particle and Nuclear Physicists*, arXiv:0803.0834, 2008.

[2] M. Kamionkowski and E. D. Kovetz, *The Quest for B Modes from Inflationary Gravitational Waves*, Annual Review of Astronomy and Astrophysics, vol. 54, pp. 227–269, 2016.

[3] P. A. R. Ade et al. (BICEP2/Keck Collaboration), *Constraints on Primordial Gravitational Waves using Planck, WMAP, and BICEP2/Keck Observations*, Physical Review Letters, 2018.

[4] J. Borrill et al., *Full-sky Models of Galactic Microwave Emission and Polarization at Sub-arcminute Scales for the Python Sky Model*, arXiv:2502.20452, 2025.